VISTA: Visual-Textual Knowledge Graph Representation Learning

Jaejun Lee Chanyoung Chung Hochang Lee
Sungho Jo Joyce Jiyoung Whang[*]
School of Computing, KAIST
{jjlee98, chanyoung.chung, hochang.lee91, shjo, jjwhang}@kaist.ac.kr

Abstract

Knowledge graphs represent human knowledge using triplets composed of entities and relations. While most existing knowledge graph embedding methods only consider the structure of a knowledge graph, a few recently proposed multimodal methods utilize images or text descriptions of entities in a knowledge graph. In this paper, we propose visual-textual knowledge graphs (VTKGs), where not only entities but also triplets can be explained using images, and both entities and relations can accompany text descriptions. By compiling visually expressible commonsense knowledge, we construct new benchmark datasets where triplets themselves are explained by images, and the meanings of entities and relations are described using text. We propose VISTA, a knowledge graph representation learning method for VTKGs, which incorporates the visual and textual representations of entities and relations using entity encoding, relation encoding, and triplet decoding transformers. Experiments show that VISTA outperforms state-of-the-art knowledge graph completion methods in real-world VTKGs.

1 Introduction

Knowledge graphs provide diverse human knowledge in a structured form, representing each fact as a triplet consisting of entities and a relation. Knowledge graph representation learning methods (Ji et al., 2022) aim to convert the entities and relations into a set of representation vectors which can be utilized in predicting missing triplets or in other applications such as commonsense reasoning (Lin et al., 2019) and question answering models (Liu et al., 2020). While most existing knowledge graph embedding methods focus solely on the structure of a knowledge graph to learn the representations (Lacroix et al., 2018; Sun et al., 2019), using additional images or text descriptions can result in much better representations. A few

[*]Corresponding author

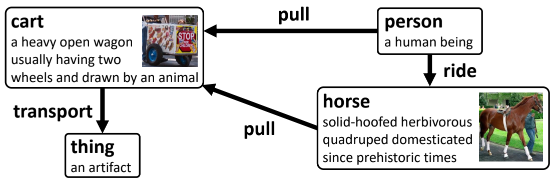
cart
a heavy open wagon usually having two wheels and drawn by an animal
pull
person
a human being
ride
transport
pull
horse
solid-hoofed herbivorous quadruped domesticated since prehistoric times
thing
an artifact

(a) Existing Multimodal Knowledge Graph

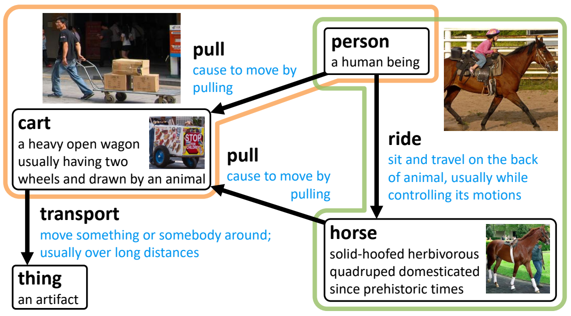
pull
cause to move by pulling
person
a human being
cart
a heavy open wagon usually having two wheels and drawn by an animal
pull
cause to move by pulling
ride
sit and travel on the back of animal, usually while controlling its motions
transport
move something or somebody around; usually over long distances
horse
solid-hoofed herbivorous quadruped domesticated since prehistoric times
thing
an artifact

(b) Visual-Textual Knowledge Graph (VTKG)

Figure 1: While existing methods assume only entities have their images and text descriptions, our VTKG additionally considers cases where a triplet itself is represented by an image, and relations have text descriptions.

recently proposed multimodal knowledge graph completion methods (Zhao et al., 2022; Li et al., 2023) consider the case where entities can have their images and text descriptions; Figure 1 (a) is a form of knowledge graph existing multimodal knowledge graph completion methods consider.

We focus on the fact that some triplets can be more intuitively expressed by their images. For example, in Figure 1 (b), ⟨person, ride, horse⟩ and ⟨person, pull, cart⟩ have images, where the triplets themselves are represented by images, providing visual insights. On the other hand, existing knowledge graphs do not provide images for triplets and may lack visually expressible triplets because they are constructed by extracting information mainly from texts. Therefore, we propose forming a knowledge graph by extracting information from images and utilizing those images to represent visual commonsense knowledge.

To this end, we compile visual phrases in triplets and their images from diverse computer vision tasks, including visual relationship detection (Lu et al., 2016), human-object interaction detection (Chao et al., 2018), and visual knowledge extraction (Sadeghi et al., 2015). We propose Visual-Textual Knowledge Graphs (VTKGs) where the entities and triplets can be represented by images, and the entities and relations have their text descriptions as shown in Figure 1 (b). We build new VTKG benchmark datasets containing visually expressible commonsense knowledge, the entities' and triplets' images, and detailed descriptions of the entities and relations.

To learn representations of entities and relations in VTKGs, we propose the **VIS**ual-**T**extu**A**l (VISTA) knowledge graph representation learning method that utilizes not only the structure of a visual-textual knowledge graph but also the visual and textual features extracted from images and text descriptions. In particular, when a triplet is provided with an image, VISTA learns the visual representation of the relation in the given triplet. The resulting visual representation of the relation is also utilized when the relation appears in other triplets, which enhances the entire representation learning process. To the best of our knowledge, VISTA is the first knowledge graph representation learning method that learns the visual representations for visually expressible relations. We design VISTA by proposing three transformers: entity encoding, relation encoding, and triplet decoding transformers. The entity and relation encoding transformers represent entities and relations using their visual and textual feature vectors, whereas the triplet decoding transformer predicts a missing entity in a triplet using a masking scheme. Experimental results on four real-world datasets demonstrate that VISTA outperforms 10 different state-of-the-art knowledge graph completion methods. Our datasets and codes are available at `https://github.com/bdi-lab/VISTA`.

2 Related Work

Visual Commonsense Reasoning There have been some attempts to extract visual knowledge from images by using visually verifiable relations (Sadeghi et al., 2015; Chen et al., 2013). However, they were not studied in the context of multimodal knowledge graph representation learning, and some datasets are not accessible now. More recently, the Visual Genome dataset (Krishna et al., 2017) has been released, where diverse computer vision datasets are merged. However, this dataset contains heterogeneous information which is not in the form of triplets or is hard to be considered as commonsense knowledge. On the other hand, our VTKG datasets provide visual commonsense knowledge in the form of triplets with images and can seamlessly enlarge existing knowledge bases. We believe our work can be utilized in visual commonsense reasoning (Zellers et al., 2019) and visual question answering (VQA) (Antol et al., 2015).

Knowledge Integration Ilievski et al. have attempted to examine the characteristics of information from different sources by manually categorizing the kind of knowledge (Ilievski et al., 2021). From a multimodal learning point of view, adding different modalities to existing knowledge bases has been considered (Zhu et al., 2022), e.g., adding images or texts to entities in a knowledge graph. Different from these approaches, our VTKGs are proposed to represent visually expressible knowledge, and our benchmark datasets are created by a fine-level alignment of entities and relations from different sources using WordNet synsets (Miller, 1995). Details are described in Section 3.2.

Multimodal Knowledge Graph Completion While some knowledge graph embedding methods utilize images of entities (Xie et al., 2017; Wang et al., 2021; Oñoro-Rubio et al., 2019; Liu et al., 2019), some recently proposed multimodal methods consider both images and text descriptions of entities (Pezeshkpour et al., 2018; Wang et al., 2019). For example, MoSE (Zhao et al., 2022) and IMF (Li et al., 2023) learn modality-specific representations and make predictions using the representations from different modalities. Also, OTKGE (Cao et al., 2022) proposes an optimal transport to align multi-modal embeddings, while MKGformer (Chen et al., 2022) conducts multi-level fusion using a hybrid transformer. Unlike VISTA, all these existing methods assume that only entities can have images or descriptions and do not consider the cases where an image represents a triplet itself or relations have descriptions.

3 Visual-Textual Knowledge Graphs

We describe how we collect visual commonsense knowledge and create VTKG benchmark datasets.

	$\|\mathcal{V}\|$	$\|\mathcal{R}\|$	$\|\mathcal{T}\|$	$\|\mathcal{I}_{\text{ent}}\|$	$\|\mathcal{I}_{\text{tri}}\|$	$\|\mathcal{D}_{\text{ent}}\|$	$\|\mathcal{D}_{\text{rel}}\|$	VTKG-I	VTKG-C
VRD	130	88	842	14,945	10,372	129	80	✓	✓
UnRel	31	19	44	1,636	939	31	18	✓	✓
HICO-DET	96	157	516	232,830	129,936	92	155	✓	✓
VisKE	605	563	2,422	0	0	591	552		✓
ConceptNetW	6,260	2,421	14,919	0	0	5,922	2,205		✓
WN18RR++	41,105	11	93,003	70,349	0	41,105	0		✓

Table 1: The original sources of our two VTKG datasets. The first four rows are datasets representing visual commonsense knowledge, and the last two rows are knowledge bases.

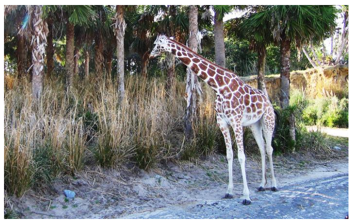

Figure 2: Visual Relationship Detection. Given an image, a short visual phrase is created using a triplet.

3.1 Representing Visual Commonsense Knowledge as Triplets and Images

There can be many different design choices for extracting information from images, depending on the type of information we want to extract. Among others, we look into computer vision tasks returning a visual phrase in the form of ⟨object$_1$, predicate, object$_2$⟩. We assemble visual commonsense knowledge using four benchmark datasets from three different computer vision tasks: VRD (Lu et al., 2016) and UnRel (Peyre et al., 2017) for visual relationship detection, HICO-DET (Chao et al., 2018) for human-object interaction detection, and VisKE (Sadeghi et al., 2015) for visual knowledge extraction. All these tasks return a short visual phrase in the triplet format to describe a given image. For example, Figure 2 shows an output of visual relationship detection. Among the four datasets, VRD, UnRel, and HICO-DET provide the triplets with images, whereas VisKE only provides triplets but not images. When collecting the visual phrases from these datasets, we filter out image-specific phrases that are hard to be considered as commonsense knowledge, e.g., ⟨dog, `on_the_right_of`, vase⟩.

3.2 Defining and Creating VTKGs

We define a VTKG as $G = (\mathcal{V}, \mathcal{R}, \mathcal{T}, \mathcal{I}, \mathcal{D})$ where $\mathcal{V}$ is a set of entities, $\mathcal{R}$ is a set of relations, $\mathcal{T}$ is a set of triplets, $\mathcal{I}$ is a set of images, and $\mathcal{D}$ is a set of text descriptions. Since an image can be attached to an entity or a triplet, $\mathcal{I} = \mathcal{I}_{\text{ent}} \cup \mathcal{I}_{\text{tri}}$ where $\mathcal{I}_{\text{ent}}$ indicates a set of images attached to entities and $\mathcal{I}_{\text{tri}}$ is a set of images attached to triplets. Also, $\mathcal{D} = \mathcal{D}_{\text{ent}} \cup \mathcal{D}_{\text{rel}}$ where $\mathcal{D}_{\text{ent}}$ and $\mathcal{D}_{\text{rel}}$ indicate the descriptions of entities and relations, respectively. Throughout the paper, we use script upper cases for sets, boldfaced upper cases for matrices, and boldfaced lower cases for vectors.

To create VTKG datasets, we use well-known knowledge bases, ConceptNet (Speer et al., 2017) and WN18RR (Dettmers et al., 2018). We note that some tail entities in ConceptNet include predicates. For example, ⟨`spider`, `CapableOf`, `kill_a_fly`⟩ should be converted to ⟨`spider`, `kill`, `fly`⟩ to be consistent with other triplets in the other datasets; this consistency is important because we combine triplets from different sources to create our VTKG datasets where the same entities and relations should be appropriately aligned across different datasets. We manually inspected the triplets in ConceptNet for three weeks, resulting in the **ConceptNetW** dataset, which is a subset of ConceptNet, containing 14,919 triplets. On the other hand, in the original WN18RR, the entity types are missing. Thus, some entities are not mapped into a unique synset ID which is defined in WordNet (Miller, 1995), resulting in incorrectly representing different entities as one entity. To fix this, we manually mapped those entities to one of the five types: noun, verb, adjective, adjective satellite, and adverb. The resulting dataset is **WN18RR++**.

Using the visual commonsense knowledge datasets and knowledge bases, we create two VTKG datasets shown in Table 1. In **VTKG-I**, we combine visual commonsense datasets where all triplets have their images. In **VTKG-C**, we merge all visual commonsense datasets and two knowledge bases, ConceptNetW and WN18RR++.

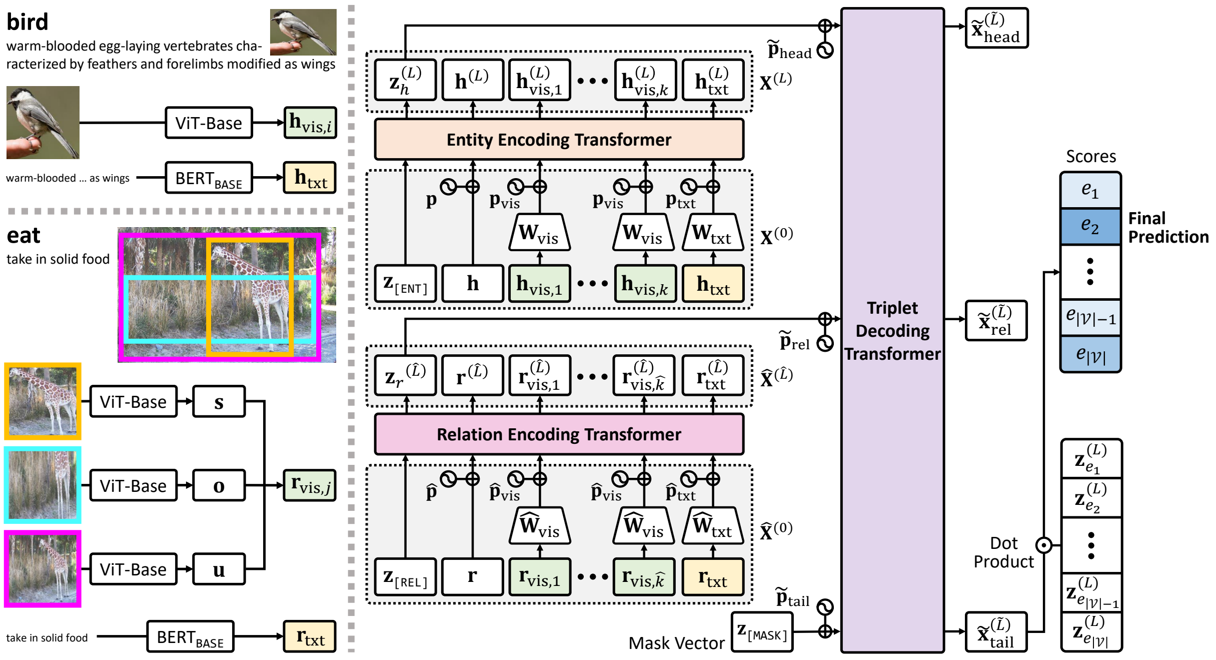
bird
warm-blooded egg-laying vertebrates characterized by feathers and forelimbs modified as wings
ViT-Base
$\mathbf{h}_{\text{vis},i}$
warm-blooded ... as wings
BERT$_{\text{BASE}}$
$\mathbf{h}_{\text{txt}}$
eat
take in solid food
ViT-Base
$\mathbf{s}$
$\mathbf{o}$
$\mathbf{u}$
$\mathbf{r}_{\text{vis},j}$
take in solid food
$\mathbf{r}_{\text{txt}}$
Entity Encoding Transformer
Relation Encoding Transformer
Triplet Decoding Transformer
$\mathbf{X}^{(L)}$
$\mathbf{X}^{(0)}$
$\widehat{\mathbf{X}}^{(\widehat{L})}$
$\widehat{\mathbf{X}}^{(0)}$
$\widetilde{\mathbf{p}}_{\text{head}}$
$\widetilde{\mathbf{p}}_{\text{rel}}$
$\widetilde{\mathbf{p}}_{\text{tail}}$
$\widetilde{\mathbf{x}}^{(\widetilde{L})}_{\text{head}}$
$\widetilde{\mathbf{x}}^{(\widetilde{L})}_{\text{rel}}$
$\widetilde{\mathbf{x}}^{(\widetilde{L})}_{\text{tail}}$
Mask Vector
$\mathbf{z}_{\texttt{[MASK]}}$
$\mathbf{z}_{\texttt{[ENT]}}$
$\mathbf{z}_{\texttt{[REL]}}$
Scores
Final Prediction
Dot Product
e_1 e_2 $e_{|\mathcal{V}|-1}$ $e_{|\mathcal{V}|}$

Figure 3: Overview of VISTA. We extract visual and textual features using ViT-Base and BERT$_{\text{BASE}}$. The entity and relation encoding transformers compute the entity and relation representations, respectively. The resulting representations are fed to the triplet decoding transformer, which predicts a missing entity in a triplet.

Constructing VTKG datasets requires much more effort than simply unioning the triplets because the triplets from different sources are usually written using different vocabularies, and the semantics of the same word should be determined depending on the context. For example, the same concept can be written using different words, e.g., `human` or `person`. Also, the same word can indicate different meanings depending on the context, e.g., ⟨`diamond`, `scratch`, `glass`⟩ or ⟨`bartender`, `fill`, `glass`⟩. To refine the expressions, we mapped each entity and relation into a synset provided in WordNet. This mapping requires us to select the most appropriate synset of each word in a triplet by examining the meaning of each synset and the semantics of the word in context. **We replaced the entity and the relation with the corresponding synset ID so that all triplets are rephrased using the synsets defined in WordNet**. In this way, we consolidated the vocabularies used in VRD, UnRel, HICO-DET, VisKE, and ConceptNetW. Details about this process are described in Appendix A. Since WN18RR++ is a subset of WordNet, it did not require this post-processing.

4 VISTA: Learning Representations in Visual-Textual Knowledge Graphs

We propose VISTA shown in Figure 3. We extract visual and textual features from images and text descriptions using pretrained ViT (Dosovitskiy et al., 2021) and BERT (Devlin et al., 2019). By utilizing the extracted features, VISTA learns representations of entities and relations, which are computed by the entity and relation encoding transformers, respectively. Based on the resulting entity and relation representations, VISTA predicts a missing entity in a triplet using the triplet decoding transformer.

4.1 Extracting Visual and Textual Features

In VTKGs, images can be associated with an entity or a triplet. To extract visual features from the images, we employ ViT pretrained on ImageNet-21k (Deng et al., 2009). We resize an input of ViT-Base as 224×224 and consider the final hidden state corresponding to `[class]` token as the visual feature vector. If an entity has multiple images, the entity can have multiple visual feature vectors, one from each image. In practice, we select the top k images per entity by computing pairwise dot product similarities of the visual feature vectors.

When an image is given for a triplet $\langle s, r, o \rangle$, we first extract the visual features of entities, s and o, by cropping bounding boxes, each of which contains s and o and feeding each bounding box to ViT-Base. Let $\mathbf{s}$ and $\mathbf{o}$ denote the resulting vectors. To consider the visual attribute of relation r, we define the minimal union bounding box that contains both entities s and o and compute the visual feature vector $\mathbf{u}$ by feeding this bounding box to ViT-Base. Then, we define $\mathbf{r}_{\text{vis}} = [\mathbf{s}; \mathbf{o}; \mathbf{u}]$ where ; is a vertical concatenation, $\mathbf{s}, \mathbf{o}, \mathbf{u} \in \mathbb{R}^{d_{\text{vis}}}$, and $d_{\text{vis}} = 768$. The visual representation vector of r is computed by learning a projection matrix acting on $\mathbf{r}_{\text{vis}}$. Details are described in Section 4.3. For each relation, we select the top $\hat{k}$ images based on the pairwise dot product similarities of the $\mathbf{r}_{\text{vis}}$ values.

To extract textual features from descriptions, we employ the pretrained BERT. For each given text description of an entity or a relation, we first tokenize the description, feed the tokenized sequence to $\text{BERT}_{\text{BASE}}$, and use the final hidden state corresponding to `[CLS]` token as the textual feature vector. For entities and relations without descriptions, we feed their labels in natural language to $\text{BERT}_{\text{BASE}}$. The dimension of a textual feature vector is set to $d_{\text{txt}} = 768$.

4.2 Entity Encoding Transformer

Let us consider an entity h with k visual features, $\mathbf{h}_{\text{vis},1}, \cdots, \mathbf{h}_{\text{vis},k} \in \mathbb{R}^{d_{\text{vis}}}$, and the textual feature $\mathbf{h}_{\text{txt}} \in \mathbb{R}^{d_{\text{txt}}}$. The input of the entity encoding transformer is defined by

$$\begin{aligned}\mathbf{X}^{(0)} =& \Big[\mathbf{z}_{\texttt{[ENT]}} \| (\mathbf{h} + \mathbf{p}) \| (\mathbf{W}_{\text{vis}}\mathbf{h}_{\text{vis},1} + \mathbf{p}_{\text{vis}}) \| \cdots \\ & \| (\mathbf{W}_{\text{vis}}\mathbf{h}_{\text{vis},k} + \mathbf{p}_{\text{vis}}) \| (\mathbf{W}_{\text{txt}}\mathbf{h}_{\text{txt}} + \mathbf{p}_{\text{txt}})\Big] \\ =& \Big[\mathbf{z}_h^{(0)} \| \mathbf{h}^{(0)} \| \mathbf{h}_{\text{vis},1}^{(0)} \| \cdots \| \mathbf{h}_{\text{vis},k}^{(0)} \| \mathbf{h}_{\text{txt}}^{(0)}\Big]\end{aligned}$$

where $\mathbf{z}_{\texttt{[ENT]}} \in \mathbb{R}^d$ is a learnable vector that is shared across all entities, d is the dimension of a representation vector, $\mathbf{h} \in \mathbb{R}^d$ is a learnable vector for h, $\mathbf{W}_{\text{vis}} \in \mathbb{R}^{d \times d_{\text{vis}}}$ and $\mathbf{W}_{\text{txt}} \in \mathbb{R}^{d \times d_{\text{txt}}}$ are learnable projection matrices for converting the visual and textual features to their representation vectors, respectively, $\mathbf{p}, \mathbf{p}_{\text{vis}}, \mathbf{p}_{\text{txt}} \in \mathbb{R}^d$ are the positional encodings of the learnable vector, visual representation vectors, and the textual representation vector, respectively, and $\|$ denotes a horizontal concatenation. After L transformer encoder layers (Vaswani et al., 2017), we get the final representation matrix

$$\mathbf{X}^{(L)} = \Big[\mathbf{z}_h^{(L)} \| \mathbf{h}^{(L)} \| \mathbf{h}_{\text{vis},1}^{(L)} \| \cdots \| \mathbf{h}_{\text{vis},k}^{(L)} \| \mathbf{h}_{\text{txt}}^{(L)}\Big]$$

and we use $\mathbf{z}_h^{(L)}$ as the representation vector of the entity h.

4.3 Relation Encoding Transformer

Given a relation r, consider $\mathbf{r}_{\text{vis},1}, \cdots, \mathbf{r}_{\text{vis},\hat{k}} \in \mathbb{R}^{3d_{\text{vis}}}$ described in Section 4.1. Let us consider images containing the relation r. Specifically, consider the j-th image containing a triplet $\langle s_j, r, o_j \rangle$. Recall that $\mathbf{r}_{\text{vis},j}$ is created by concatenating the visual features of s_j, o_j, and the union bounding box containing s_j and o_j. We compute the initial visual representation vector of r for the j-th image by $\widehat{\mathbf{W}}_{\text{vis}}\mathbf{r}_{\text{vis},j}$ where a learnable projection matrix $\widehat{\mathbf{W}}_{\text{vis}}$ is introduced. A visual representation vector of r is learned per image while sharing the projection matrix. The way we compute the visual representation of r can be considered as a generalization of UVTransE (Hung et al., 2021) since $\widehat{\mathbf{W}}_{\text{vis}}$ allows flexible operations between the feature vectors of s, o, and their union bounding box, whereas UVTransE employs a fixed constraint. On the other hand, let $\widehat{\mathbf{W}}_{\text{txt}} \in \mathbb{R}^{d \times d_{\text{txt}}}$ be a learnable matrix for converting the textual feature vector $\mathbf{r}_{\text{txt}}$ of r to its textual representation vector.

The input of the relation encoding transformer is

$$\begin{aligned}\widehat{\mathbf{X}}^{(0)} =& \Big[\mathbf{z}_{\texttt{[REL]}} \| (\mathbf{r} + \widehat{\mathbf{p}}) \| (\widehat{\mathbf{W}}_{\text{vis}}\mathbf{r}_{\text{vis},1} + \widehat{\mathbf{p}}_{\text{vis}}) \| \cdots \\ & \| (\widehat{\mathbf{W}}_{\text{vis}}\mathbf{r}_{\text{vis},\hat{k}} + \widehat{\mathbf{p}}_{\text{vis}}) \| (\widehat{\mathbf{W}}_{\text{txt}}\mathbf{r}_{\text{txt}} + \widehat{\mathbf{p}}_{\text{txt}})\Big] \\ =& \Big[\mathbf{z}_r^{(0)} \| \mathbf{r}^{(0)} \| \mathbf{r}_{\text{vis},1}^{(0)} \| \cdots \| \mathbf{r}_{\text{vis},\hat{k}}^{(0)} \| \mathbf{r}_{\text{txt}}^{(0)}\Big]\end{aligned}$$

where $\mathbf{z}_{\texttt{[REL]}} \in \mathbb{R}^d$ is a learnable vector that is shared across all relations, $\mathbf{r} \in \mathbb{R}^d$ is a learnable vector for r, $\widehat{\mathbf{p}}, \widehat{\mathbf{p}}_{\text{vis}}, \widehat{\mathbf{p}}_{\text{txt}} \in \mathbb{R}^d$ are the positional encodings of the learnable vector, visual representation vectors, and the textual representation vector, respectively. After $\widehat{L}$ transformer encoder layers, we get the final representation matrix

$$\widehat{\mathbf{X}}^{(\widehat{L})} = \Big[\mathbf{z}_r^{(\widehat{L})} \| \mathbf{r}^{(\widehat{L})} \| \mathbf{r}_{\text{vis},1}^{(\widehat{L})} \| \cdots \| \mathbf{r}_{\text{vis},\hat{k}}^{(\widehat{L})} \| \mathbf{r}_{\text{txt}}^{(\widehat{L})}\Big]$$

and we use $\mathbf{z}_r^{(\widehat{L})}$ as the representation vector of the relation r.

4.4 Triplet Decoding Transformer

Given a triplet $\langle h, r, ? \rangle$, the triplet decoding transformer predicts the missing entity using $\mathbf{z}_h^{(L)}$, $\mathbf{z}_r^{(\widehat{L})}$, and a learnable mask vector $\mathbf{z}_{\texttt{[MASK]}} \in \mathbb{R}^d$. The input of the triplet decoding transformer is

$$\begin{aligned}\widetilde{\mathbf{X}}^{(0)} =& \big[(\mathbf{z}_h^{(L)} + \widetilde{\mathbf{p}}_{\text{head}}) \| (\mathbf{z}_r^{(\widehat{L})} + \widetilde{\mathbf{p}}_{\text{rel}}) \| (\mathbf{z}_{\texttt{[MASK]}} + \widetilde{\mathbf{p}}_{\text{tail}})\big] \\ =& \big[\widetilde{\mathbf{x}}_{\text{head}}^{(0)} \| \widetilde{\mathbf{x}}_{\text{rel}}^{(0)} \| \widetilde{\mathbf{x}}_{\text{tail}}^{(0)}\big]\end{aligned}$$

where $\widetilde{\mathbf{p}}_{\text{head}}, \widetilde{\mathbf{p}}_{\text{rel}}, \widetilde{\mathbf{p}}_{\text{tail}} \in \mathbb{R}^d$ are the positional encodings of the head entity, relation, and tail entity, respectively. After applying $\widetilde{L}$ transformer encoder layers, we have

$$\widetilde{\mathbf{X}}^{(\widetilde{L})} = [\widetilde{\mathbf{x}}_{\text{head}}^{(\widetilde{L})} \| \widetilde{\mathbf{x}}_{\text{rel}}^{(\widetilde{L})} \| \widetilde{\mathbf{x}}_{\text{tail}}^{(\widetilde{L})}]$$

and calculate the score y_j of an entity e_j by $y_j = \widetilde{\mathbf{x}}_{\text{tail}}^{(\widetilde{L})} \cdot \mathbf{z}_{e_j}^{(L)}$ where $\mathbf{z}_{e_j}^{(L)}$ is the representation vector of e_j computed from the entity encoding transformer. We predict the missing entity to be the entity with the highest score. Similarly, we can also make a prediction for $\langle ?, r, t \rangle$. We use the cross entropy loss in our implementation.

5 Experiments

We evaluate the performance of VISTA using four real-world datasets by comparing it to 10 different knowledge graph completion methods. We implement VISTA using PyTorch (Paszke et al., 2019) with the Adam optimizer (Kingma and Ba, 2015). We apply dropout (Srivastava et al., 2014) and use the cosine annealing scheduler (Loshchilov and Hutter, 2017).

5.1 Datasets and Experimental Setup

We use four datasets shown in Table 2; VTKG-I and VTKG-C are real-world VTKG datasets introduced in Section 3.2. While WN18 (Bordes et al., 2013) and FB15K237 (Toutanova and Chen, 2015) are benchmark datasets used in other multimodal knowledge graph completion research (Zhao et al., 2022; Chen et al., 2022), WN18 has a test leakage issue, and WN18RR (Dettmers et al., 2018) has been proposed to resolve the issue. In our experiments, we use WN18RR++ which is the fixed version of WN18RR as described in Section 3.2. Our VTKG datasets include images for triplets and entities, whereas the existing benchmark datasets provide images only for entities.

We use ten different baseline methods: ANALOGY (Liu et al., 2017), ComplEx-N3 (Lacroix et al., 2018), RotatE (Sun et al., 2019), PairRE (Chao et al., 2021), RSME (Wang et al., 2021), TransAE (Wang et al., 2019), MKGformer (Chen et al., 2022), OTKGE (Cao et al., 2022), MoSE (Zhao et al., 2022), and IMF (Li et al., 2023). The first four methods are knowledge graph embedding methods only considering the structure of the given knowledge graph, whereas RSME can deal with images of entities. The rest five methods are multimodal knowledge graph representation learning methods that consider images and text descriptions of entities. We run MoSE with three different options, denoted by MoSE-AI, MoSE-BI, and MoSE-MI. Details about running the baseline methods are described in Appendix B.

	$\lvert\mathcal{V}\rvert$	$\lvert\mathcal{R}\rvert$	$\lvert\mathcal{T}\rvert$	$\lvert\mathcal{I}\rvert$	$\lvert\mathcal{D}\rvert$
VTKG-I	181	217	1,316	390,658	383
VTKG-C	43,267	2,731	111,491	461,007	45,401
WN18RR++	41,105	11	93,003	70,349	41,105
FB15K237	14,541	237	310,116	145,944	14,515

Table 2: Statistic of Datasets

We divide the training, valid, and test sets with a ratio of 8:1:1 for VTKGs; we use the provided split for the existing benchmark datasets. When training a model using triplets' images, we only use the images associated with the triplets in a training set. For knowledge graph completion in the VTKG datasets, if the task is to predict a head or a tail entity in $\langle h, r, t \rangle$, we do not provide any image associated with the triplet $\langle h, r, t \rangle$ to a model at a testing time because its image can directly hint at the missing entity. From training to testing, we never use images of test triplets. We explain the hyperparameters of VISTA in Appendix C. For fair comparisons, we set $d = 256$ on all datasets for all methods except MKGformer; the dimension in MKGformer is fixed to $d = 768$ since it directly uses ViT and BERT.

5.2 Knowledge Graph Completion

We evaluate the knowledge graph completion performance using MR (↓), MRR (↑), and Hit@N (↑, N=1,3,10) in Table 3. The best results are boldfaced, and the second-best results are underlined. Overall, VISTA significantly outperforms all baseline methods. While the second-best method varies depending on the dataset and the metric, VISTA consistently shows the best performance. In VTKG-I and VTKG-C, there is a substantial performance gap between VISTA and the best baseline method in all metrics. While VISTA utilizes relations' visual representation vectors and their text descriptions, none of the baseline methods is capable of dealing with them. This difference attributes to the performance gap between VISTA and the baseline methods since the VTKG datasets include visually expressible relations provided by images of triplets and abundant text descriptions for relations. On the other hand, WN18RR++ and

	VTKG-I					VTKG-C				
	MR	MRR	Hit@1	Hit@3	Hit@10	MR	MRR	Hit@1	Hit@3	Hit@10
ANALOGY	39.5	0.3040	0.2328	0.3015	0.4466	10392.1	0.2963	0.2609	0.3180	0.3532
ComplEx-N3	31.8	0.3911	0.3168	0.4046	0.5191	3668.0	0.3944	0.3515	0.4079	0.4815
RotatE	24.5	0.3131	0.2099	0.3473	0.5267	4121.2	0.3893	0.3473	0.4062	0.4704
PairRE	20.9	0.4104	0.3015	0.4504	0.6145	2736.8	0.3876	0.3431	0.4013	0.4782
RSME	32.0	0.4027	0.3321	0.4122	0.5573	4401.4	0.3942	0.3513	0.4096	0.4776
TransAE	19.5	0.2437	0.0687	0.3092	0.6374	3063.3	0.0751	0.0053	0.1053	0.2072
MKGformer	29.9	0.3884	0.3397	0.3740	0.4885	668.5	0.4227	0.3531	0.4487	0.5580
OTKGE	27.5	0.4278	0.3588	0.4466	0.5458	2606.8	0.3939	0.3446	0.4152	0.4881
MoSE-AI	22.5	0.4306	0.3473	0.4466	0.6221	854.3	0.3929	0.3186	0.4301	0.5210
MoSE-BI	23.7	0.4297	0.3473	0.4466	0.6221	615.9	0.3933	0.2825	0.4578	0.5864
MoSE-MI	34.0	0.4235	0.3397	0.4504	0.6107	527.0	0.4056	0.2913	0.4762	0.5977
IMF	35.6	0.4184	0.3282	0.4656	0.5649	2951.6	0.4116	0.3706	0.4261	0.4935
VISTA	**17.3**	**0.4650**	**0.3626**	**0.5076**	**0.6641**	**220.8**	**0.4675**	**0.3918**	**0.4961**	**0.6157**
	WN18RR++					FB15K237				
	MR	MRR	Hit@1	Hit@3	Hit@10	MR	MRR	Hit@1	Hit@3	Hit@10
ANALOGY	7453.8	0.4128	0.3969	0.4175	0.4438	371.9	0.2420	0.1516	0.2677	0.4301
ComplEx-N3	3545.0	0.4745	0.4292	0.4895	0.5675	172.7	0.3510	0.2584	0.3847	0.5391
RotatE	5946.1	0.4606	0.4274	0.4754	0.5230	246.1	0.3099	0.2183	0.3433	0.4932
PairRE	3676.2	0.4529	0.4127	0.4663	0.5351	184.3	0.3326	0.2399	0.3675	0.5193
RSME	4062.1	0.4567	0.4175	0.4751	0.5300	174.9	0.3445	0.2523	0.3780	0.5286
TransAE	2308.2	0.0900	0.0040	0.1291	0.2511	234.6	0.2122	0.1432	0.2267	0.3459
MKGformer	352.3	0.5308	0.4697	0.5557	0.6560	297.6	0.3095	0.2278	0.3356	0.4740
OTKGE	1993.1	0.4327	0.3722	0.4663	0.5407	168.1	0.3411	0.2511	0.3739	0.5192
MoSE-AI	303.2	0.4857	0.4255	0.5094	0.5996	149.1	0.3247	0.2384	0.3532	0.4965
MoSE-BI	**108.0**	0.5026	0.4151	0.5461	0.6670	132.3	0.3466	0.2570	0.3755	0.5303
MoSE-MI	205.3	0.4969	0.4026	0.5466	0.6681	148.9	0.3275	0.2416	0.3568	0.4984
IMF	3774.0	0.4749	0.4397	0.4845	0.5469	151.8	0.3677	0.2735	0.4040	0.5573
VISTA	177.6	**0.5526**	**0.4871**	**0.5799**	**0.6755**	**114.2**	**0.3808**	**0.2873**	**0.4158**	**0.5718**

Table 3: Knowledge Graph Completion Performance. VISTA outperforms all baseline methods in all datasets.

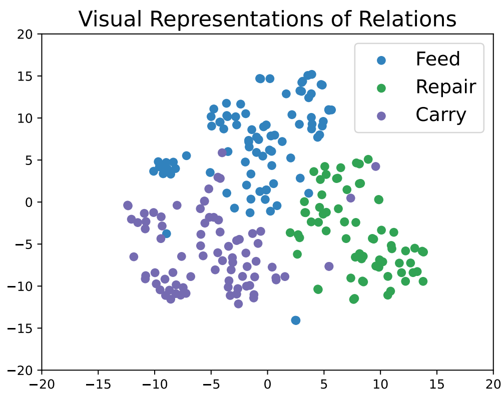

Figure 4: Visual representation vectors of relations, `Feed`, `Repair`, and `Carry`, where the vectors are computed on images of triplets containing the three relations.

FB15K237 do not include images for triplets and descriptions for relations. In WN18RR++, even though VISTA shows the second-best performance in MR, the MRR, Hit@1, Hit@3, and Hit@10 scores of VISTA are better than any other methods. In FB15K237, VISTA outperforms all baseline methods.

5.3 Qualitative Analysis

We conduct qualitative analysis using VISTA trained on VTKG-C. In Section 4.3, VISTA learns $\widehat{\mathbf{W}}_{\text{vis}}$ to compute the visual representation vectors of relations from images. Figure 4 shows the visual representation vectors of three relations, `Feed`, `Repair`, and `Carry`, visualized by t-SNE. From a testing set, we select images corresponding to triplets containing the three relations and compute the visual representation vectors using the learned $\widehat{\mathbf{W}}_{\text{vis}}$. We see that the visual representations corresponding to the same relation are well clustered even though VISTA computes them based on unseen images and triplets during training.

We qualitatively compare the representation vectors created by BERT (Devlin et al., 2019), ViT (Dosovitskiy et al., 2021), and VISTA in VTKG-C. Given a query entity (or a relation), we retrieve the top 3 similar entities (or relations) to the query based on the representation vectors returned by BERT, ViT, and VISTA. Table 4 shows the results where the query entities are `jar` and `dark_red`, and the query relations are `have` and `buy`. We see that BERT returns some abstract con-

Query		BERT	ViT	VISTA
jar	1	eyelet	lid	bucket
	2	tent	top	barrel
	3	gravy_boat	coquilla_nut	bowl
dark_red	1	incense	leisure_wear	orange
	2	coloring	sportswear	red
	3	buffer	sweatshirt	crimson
have	1	move	straddle	keep
	2	influence	hop_on	hold
	3	begin	inspect	incorporate
buy	1	stipulate	pluck	share
	2	incorporate	jab	price
	3	use	own	trade

Table 4: Top three similar entities or relations to the query in VTKG-C based on the representation vectors created by BERT, ViT, and VISTA.

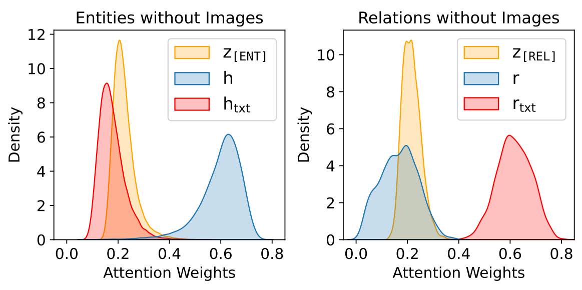

(a) Attention weights in the entity and relation encoding transformers for entities and relations without images

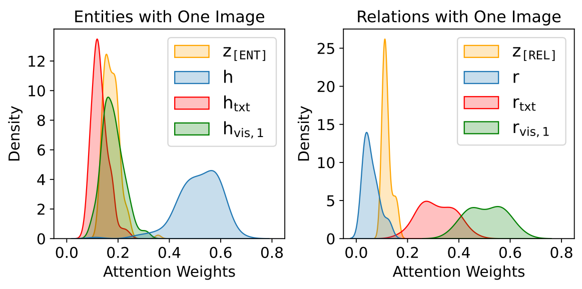

(b) Attention weights in the entity and relation encoding transformers for entities and relations with one image

Figure 5: Distributions of attention weights in the entity and relation encoding transformers.

cepts, e.g., `incense` and `influence`, whereas ViT returns visually expressible concepts, e.g., `lid` and `straddle`. VISTA successfully returns the most semantically close entities and relations to the queries by utilizing both texts and images.

As described in Section 4.2, the entity encoding transformer of VISTA learns the representation vector of each entity based on $\mathbf{z}_{\texttt{[ENT]}}$, $\mathbf{h}$, $\mathbf{h}_{\text{vis},1}$, $\cdots$, $\mathbf{h}_{\text{vis},k}$, and $\mathbf{h}_{\text{txt}}$. Similarly, the relation encoding transformer learns the representation vector of a relation based on $\mathbf{z}_{\texttt{[REL]}}$, $\mathbf{r}$, $\mathbf{r}_{\text{vis},1}$, $\cdots$, $\mathbf{r}_{\text{vis},\hat{k}}$, and $\mathbf{r}_{\text{txt}}$ as described in Section 4.3. To analyze the contribution of each of these terms, we visualize the attention weights using kernel density estimate plots. Figure 5 shows the distributions of the attention weights for entities and relations for (a) the case where the entities and relations do not have images and (b) the case where the entities and relations have images. When we consider the case when images are not given, textual features $\mathbf{r}_{\text{txt}}$, play the most crucial role in relations. On the other hand, in entities, the learnable vector $\mathbf{h}$ has relatively high attention weights. When images are given, the visual attributes of relations $\mathbf{r}_{\text{vis},1}$, tend to have high contributions, sometimes even exceeding the contributions of textual descriptions $\mathbf{r}_{\text{txt}}$. This verifies that learning visual representations of relations are effective in VISTA, which contributes to the performance of VISTA. For entities, the learnable vector $\mathbf{h}$ still has high importance when images are given, and the visual features $\mathbf{h}_{\text{vis},1}$ tend to have slightly higher importance than textual features $\mathbf{h}_{\text{txt}}$.

5.4 Ablation Studies

We present ablation studies of VISTA in Table 5. We show the results of VISTA using different combinations of the modalities (the "Modality" rows). Also, we show the impact of different modalities for entities (the "Entity Modality" rows) and for relations (the "Relation Modality" rows). On both VTKG-I and VTKG-C, we see that adding visual or textual features leads to better performance than the case without those features. More importantly, using all modalities presented in the last row of Table 5 (VISTA) leads to the best performance.

The impact of the visual features is more prominent on VTKG-I than on VTKG-C. To analyze it, we count the number of entities and relations with and without visual features, shown in Table 6. While all entities and relations have their visual features on VTKG-I, many entities and relations do not have visual features on VTKG-C. As a result, visual features are more important than textual features on VTKG-I, while textual features are more important than visual features on VTKG-C.

On the other hand, the performance decreases of VISTA with 'replace $\mathbf{r}_{\text{vis}}$ w/ $\mathbf{u}$' indicate that our way of constructing $\mathbf{r}_{\text{vis}}$ is more effective than just using the union bounding box of a triplet when creating a visual representation vector of r.

Furthermore, we remove or replace some components in VISTA. Specifically, for the "Encoder" part, we consider the cases where (1) we remove $\mathbf{z}_{\texttt{[ENT]}}$ and $\mathbf{z}_{\texttt{[REL]}}$, (2) we remove $\mathbf{h}$ and $\mathbf{r}$, (3) we

		VTKG-I					VTKG-C				
		MR	MRR	Hit@1	Hit@3	Hit@10	MR	MRR	Hit@1	Hit@3	Hit@10
Modality	w/o $\mathbf{h}_{\text{vis}}$, $\mathbf{h}_{\text{txt}}$, $\mathbf{r}_{\text{vis}}$, $\mathbf{r}_{\text{txt}}$	23.3	0.398	0.309	0.431	0.573	3163.9	0.365	0.325	0.381	0.441
	w/o $\mathbf{h}_{\text{vis}}$, $\mathbf{r}_{\text{vis}}$	21.0	0.442	0.347	0.454	0.645	238.7	0.456	0.383	0.481	0.601
	w/o $\mathbf{h}_{\text{txt}}$, $\mathbf{r}_{\text{txt}}$	19.5	0.453	0.363	0.473	0.634	2641.1	0.374	0.333	0.389	0.452
Entity Modality	w/o $\mathbf{h}_{\text{vis}}$, $\mathbf{h}_{\text{txt}}$	22.2	0.397	0.294	0.439	0.592	3036.6	0.366	0.327	0.382	0.440
	w/o $\mathbf{h}_{\text{vis}}$	20.5	0.415	0.305	0.454	0.622	229.1	0.457	0.383	0.484	0.603
	w/o $\mathbf{h}_{\text{txt}}$	17.2	0.459	0.359	0.496	0.664	2599.5	0.372	0.331	0.387	0.449
Relation Modality	w/o $\mathbf{r}_{\text{vis}}$, $\mathbf{r}_{\text{txt}}$	18.8	0.430	0.324	0.466	0.641	235.8	0.460	0.386	0.487	0.610
	w/o $\mathbf{r}_{\text{vis}}$	19.0	0.455	0.359	0.492	0.641	223.7	0.466	0.391	0.493	0.613
	w/o $\mathbf{r}_{\text{txt}}$	17.3	0.459	0.351	0.500	0.664	236.3	0.461	0.385	0.490	0.609
	replace $\mathbf{r}_{\text{vis}}$ w/ $\mathbf{u}$	18.3	0.433	0.336	0.458	0.649	318.1	0.416	0.341	0.445	0.557
Encoder	w/o $\mathbf{z}_{\texttt{[ENT]}}$ and $\mathbf{z}_{\texttt{[REL]}}$	18.6	0.402	0.290	0.454	0.622	316.8	0.402	0.325	0.434	0.549
	w/o $\mathbf{h}$ and $\mathbf{r}$	19.0	0.438	0.328	0.485	0.649	250.9	0.450	0.372	0.484	0.598
	w/o rel. trans.	18.4	0.417	0.302	0.473	0.622	369.3	0.389	0.312	0.420	0.538
	w/o ent. trans.	25.2	0.406	0.332	0.424	0.546	4368.7	0.362	0.319	0.377	0.444
Decoder	w/ DistMult decoder	21.0	0.391	0.282	0.416	0.634	420.6	0.420	0.357	0.438	0.542
	replace dot prod. w/ lin.	29.5	0.406	0.317	0.435	0.580	964.5	0.430	0.380	0.448	0.524
VISTA		17.3	0.465	0.363	0.508	0.664	220.8	0.467	0.392	0.496	0.616

Table 5: Ablation Studies of VISTA. The best performance is achieved when all modalities are considered. The performance of VISTA degrades when we remove any component or replace a component with other alternatives.

	VTKG-I	VTKG-C
Entities w/ $\mathbf{h}_{\text{vis}}$	181 (100%)	7,863 (18.2%)
Entities w/o $\mathbf{h}_{\text{vis}}$	0 (0%)	35,404 (81.8%)
Total	181	43,267
Relations w/ $\mathbf{r}_{\text{vis}}$	217 (100%)	217 (7.9%)
Relations w/o $\mathbf{r}_{\text{vis}}$	0 (0%)	2,514 (92.1%)
Total	217	2,731

Table 6: Entities and relations with and without visual features on VTKG-I and VTKG-C.

remove the relation encoding transformer and just leave the learnable vector $\mathbf{r}$, and (4) we remove the entity encoding transformer and just leave the learnable vector $\mathbf{h}$. At the first two rows of the "Encoder" in Table 5, we see that $\mathbf{z}_{\texttt{[ENT]}}$, $\mathbf{z}_{\texttt{[REL]}}$, $\mathbf{h}$, and $\mathbf{r}$ are all important inputs of the entity and relation encoding transformers. At the last two rows of the "Encoder" in Table 5, we note that removing either the entity encoding transformer or the relation encoding transformer greatly impacts VISTA's performance. Regarding Hit@1, removing the relation encoding transformer leads to a more critical decrease in performance than removing the entity encoding transformer. On the other hand, for the other metrics (i.e., MR, MRR, Hit@3, and Hit@10), the entity encoding transformer is more critical than the relation encoding transformer.

For the "Decoder" part, we consider the cases where (1) we replace the triplet decoding transformer with DistMult (Yang et al., 2015) and (2) we replace the dot product with a linear layer for prediction. The two rows of the "Decoder" in Table 5 indicate that making changes in the way of predicting a missing entity for knowledge graph completion leads to degrading the performance of VISTA. This validates the effectiveness of our triplet decoding transformer.

6 Conclusion & Future Work

We propose VTKGs, where visually expressible triplets are augmented by images, and both entities and relations have textual descriptions. By appropriately utilizing all this rich information, VISTA substantially outperforms 10 different state-of-the-art knowledge graph completion methods in real-world VTKG datasets. Our VTKG datasets and VISTA model can be utilized in diverse applications and scenarios (Sekuboyina et al., 2019; Kwak et al., 2022; Lee et al., 2023), including those requiring visual commonsense knowledge such as VQA (Marino et al., 2021) or scene graph generation (Chang et al., 2023; Zareian et al., 2020) and commonsense reasoning (Lin et al., 2019).

We will extend our work to hyper-relational knowledge graphs (Galkin et al., 2020; Chung et al., 2023) or bi-level knowledge graphs (Chung and Whang, 2023) where more information is added to each triplet using qualifiers, or higher-level relationships are considered to enrich information between triplets. By structuring an image or a description as auxiliary information or qualifiers, VISTA can be easily extended to hyper-relational knowledge graphs with images and texts.

Limitations

When constructing our VTKG datasets, we aligned the same entities and relations using WordNet synsets (Miller, 1995) as described in Section 3.2; and this process was manually conducted, which required much human effort. While utilizing automated tools would make the process more scalable, we could not find reliable and accurate annotation tools for our alignment task. Developing automated tools that can align triplets from different sources as precisely as human annotators will accelerate the convergence of diversely-sourced knowledge.

Our model, VISTA, comprises three transformers and thus might not be considered as lightweight compared to classical shallow encoder-based knowledge graph embedding methods such as RotatE (Sun et al., 2019) and ComplEx-N3 (Lacroix et al., 2018). However, we note that VISTA is faster than another transformer-based baseline, MKGformer; to process VTKG-C, VISTA took 3 hours, whereas MKGformer took 15 hours. We will explore how we can make our implementations more scalable and make our model lighter.

Acknowledgements

This research was partly supported by NRF grants funded by MSIT (2022R1A2C4001594 and 2018R1A5A1059921). This work was also supported by an IITP grant funded by MSIT 2022-0-00369 (Development of AI Technology to support Expert Decision-making that can Explain the Reasons/Grounds for Judgment Results based on Expert Knowledge).

References

Stanislaw Antol, Aishwarya Agrawal, Jiasen Lu, Margaret Mitchell, Dhruv Batra, Charles Lawrence Zitnick, and Devi Parikh. 2015. VQA: Visual question answering. In *Proceedings of the 2015 IEEE International Conference on Computer Vision*, pages 2425–2433.

Antoine Bordes, Nicolas Usunier, Alberto Garcia-Duran, Jason Weston, and Oksana Yakhnenko. 2013. Translating embeddings for modeling multi-relational data. In *Proceedings of the 27th Conference on Neural Information Processing Systems*, pages 2787–2795.

Zongsheng Cao, Qianqian Xu, Zhiyong Yang, Yuan He, Xiaochun Cao, and Qingming Huang. 2022. OTKGE: Multi-modal knowledge graph embeddings via optimal transport. In *Proceedings of the 36th Conference on Neural Information Processing Systems*, pages 39090–39102.

Xiaojun Chang, Pengzhen Ren, Pengfei Xu, Zhihui Li, Xiaojiang Chen, and Alex Hauptmann. 2023. A comprehensive survey of scene graphs: Generation and application. *IEEE Transactions on Pattern Analysis and Machine Intelligence*, 45(1):1–26.

Linlin Chao, Jianshan He, Taifeng Wang, and Wei Chu. 2021. PairRE: Knowledge graph embeddings via paired relation vectors. In *Proceedings of the 59th Annual Meeting of the Association for Computational Linguistics and the 11th International Joint Conference on Natural Language Processing*, pages 4360–4369.

Yu-Wei Chao, Yunfan Liu, Xieyang Liu, Huayi Zeng, and Jia Deng. 2018. Learning to detect human-object interactions. In *Proceedings of the 2018 IEEE Winter Conference on Applications of Computer Vision*, pages 381–389.

Xiang Chen, Ningyu Zhang, Lei Li, Shumin Deng, Chuanqi Tan, Changliang Xu, Fei Huang, Luo Si, and Huajun Chen. 2022. Hybrid transformer with multi-level fusion for multimodal knowledge graph completion. In *Proceedings of the 45th International ACM SIGIR Conference on Research and Development in Information Retrieval*, pages 904–915.

Xinlei Chen, Abhinav Shrivastava, and Abhinav Gupta. 2013. NEIL: Extracting visual knowledge from web data. In *Proceedings of the 2013 IEEE International Conference on Computer Vision*, pages 1409–1416.

Chanyoung Chung, Jaejun Lee, and Joyce Jiyoung Whang. 2023. Representation learning on hyper-relational and numeric knowledge graphs with transformers. In *Proceedings of the 29th ACM SIGKDD Conference on Knowledge Discovery and Data Mining*, pages 310–322.

Chanyoung Chung and Joyce Jiyoung Whang. 2023. Learning representations of bi-level knowledge graphs for reasoning beyond link prediction. In *Proceedings of the 37th AAAI Conference on Artificial Intelligence*, pages 4208–4216.

Jia Deng, Wei Dong, Richard Socher, Li-Jia Li, Kai Li, and Li Fei-Fei. 2009. ImageNet: A large-scale hierarchical image database. In *Proceedings of the 2009 IEEE Conference on Computer Vision and Pattern Recognition*, pages 248–255.

Tim Dettmers, Pasquale Minervini, Pontus Stenetorp, and Sebastian Riedel. 2018. Convolutional 2d knowledge graph embeddings. In *Proceedings of the 32nd AAAI Conference on Artificial Intelligence*, pages 1811–1818.

Jacob Devlin, Ming-Wei Chang, Kenton Lee, and Kristina Toutanova. 2019. BERT: Pre-training of deep bidirectional transformers for language understanding. In *Proceedings of the 2019 Conference of the North American Chapter of the Association* *for Computational Linguistics: Human Language Technologies, Volume 1*, pages 4171–4186.

Alexey Dosovitskiy, Lucas Beyer, Alexander Kolesnikov, Dirk Weissenborn, Xiaohua Zhai, Thomas Unterthiner, Mostafa Dehghani, Matthias Minderer, Georg Heigold, Sylvain Gelly, Jakob Uszkoreit, and Neil Houlsby. 2021. An image is worth 16x16 words: Transformers for image recognition at scale. In *Proceedings of the 9th International Conference on Learning Representations*.

Mikhail Galkin, Priyansh Trivedi, Gaurav Maheshwari, Ricardo Usbeck, and Jens Lehmann. 2020. Message passing for hyper-relational knowledge graphs. In *Proceedings of the 2020 Conference on Empirical Methods in Natural Language Processing*, pages 7346–7359.

Zih-Siou Hung, Arun Mallya, and Svetlana Lazebnik. 2021. Contextual translation embedding for visual relationship detection and scene graph generation. *IEEE Transactions on Pattern Analysis and Machine Intelligence*, 43(11):3820–3832.

Filip Ilievski, Alessandro Oltramari, Kaixin Ma, Bin Zhang, Deborah Louise McGuinness, and Pedro Szekely. 2021. Dimensions of commonsense knowledge. *Knowledge-Based Systems*, 229:107347.

Shaoxiong Ji, Shirui Pan, Erik Cambria, Pekka Marttinen, and Philip Shi lung Yu. 2022. A survey on knowledge graphs: Representation, acquisition, and applications. *IEEE Transactions on Neural Networks and Learning Systems*, 33(2):494–514.

Diederik Pieter Kingma and Jimmy Ba. 2015. Adam: A method for stochastic optimization. In *Proceedings of the 3rd International Conference on Learning Representations*.

Ranjay Krishna, Yuke Zhu, Oliver Groth, Justin Johnson, Kenji Hata, Joshua Kravitz, Stephanie Chen, Yannis Kalantidis, Li-Jia Li, David Ayman Shamma, Michael Scott Bernstein, and Li Fei-Fei. 2017. Visual Genome: Connecting language and vision using crowdsourced dense image annotations. *International Journal of Computer Vision*, 123(1):32–73.

Ji Ho Kwak, Jaejun Lee, Joyce Jiyoung Whang, and Sungho Jo. 2022. Semantic grasping via a knowledge graph of robotic manipulation: A graph representation learning approach. *IEEE Robotics and Automation Letters*, 7(4):9397–9404.

Timothee Lacroix, Nicolas Usunier, and Guillaume Obozinski. 2018. Canonical tensor decomposition for knowledge base completion. In *Proceedings of the 35th International Conference on Machine Learning*, pages 2863–2872.

Jaejun Lee, Chanyoung Chung, and Joyce Jiyoung Whang. 2023. InGram: Inductive knowledge graph embedding via relation graphs. In *Proceedings of the 40th International Conference on Machine Learning*, pages 18796–18809.

Xinhang Li, Xiangyu Zhao, Jiaxing Xu, Yong Zhang, and Chunxiao Xing. 2023. IMF: Interactive multimodal fusion model for link prediction. In *Proceedings of the ACM Web Conference 2023*, pages 2572–2580.

Bill Yuchen Lin, Xinyue Chen, Jamin Chen, and Xiang Ren. 2019. KagNet: Knowledge-aware graph networks for commonsense reasoning. In *Proceedings of the 2019 Conference on Empirical Methods in Natural Language Processing and the 9th International Joint Conference on Natural Language Processing*, pages 2829–2839.

Hanxiao Liu, Yuexin Wu, and Yiming Yang. 2017. Analogical inference for multi-relational embeddings. In *Proceedings of the 34th International Conference on Machine Learning*, pages 2168–2178.

Weijie Liu, Peng Zhou, Zhe Zhao, Zhiruo Wang, Qi Ju, Haotang Deng, and Ping Wang. 2020. K-BERT: Enabling language representation with knowledge graph. In *Proceedings of the 34th AAAI Conference on Artificial Intelligence*, pages 2901–2908.

Ye Liu, Hui Li, Alberto García-Durán, Mathias Niepert, Daniel Oñoro-Rubio, and David S. Rosenblum. 2019. MMKG: Multi-modal knowledge graphs. In *Proceedings of the 16th European Semantic Web Conference*, pages 459–474.

Ilya Loshchilov and Frank Hutter. 2017. SGDR: Stochastic gradient descent with warm restarts. In *Proceedings of the 5th International Conference on Learning Representations*.

Cewu Lu, Ranjay Krishna, Michael Bernstein, and Li Fei-Fei. 2016. Visual relationship detection with language priors. In *Proceedings of the 14th European Conference on Computer Vision*, pages 852–869.

Kenneth Marino, Xinlei Chen, Devi Parikh, Abhinav Gupta, and Marcus Rohrbach. 2021. KRISP: Integrating implicit and symbolic knowledge for open-domain knowledge-based VQA. In *Proceedings of the 2021 IEEE/CVF Conference on Computer Vision and Pattern Recognition*, pages 14106–14116.

George Armitage Miller. 1995. WordNet: a lexical database for English. *Communications of the ACM*, 38(11):39–41.

Daniel Oñoro-Rubio, Mathias Niepert, Alberto García-Durán, Roberto González-Sánchez, and Roberto Javier López-Sastre. 2019. Answering visual-relational queries in web-extracted knowledge graphs. In *Proceedings of the 1st Conference on Automated Knowledge Base Construction*.

Adam Paszke, Sam Gross, Francisco Massa, Adam Lerer, James Bradbury, Gregory Chanan, Trevor Killeen, Zeming Lin, Natalia Gimelshein, Luca Antiga, Alban Desmaison, Andreas Kopf, Edward Yang, Zachary DeVito, Martin Raison, Alykhan Tejani, Sasank Chilamkurthy, Benoit Steiner, Lu Fang, Junjie Bai, and Soumith Chintala. 2019. PyTorch:

An imperative style, high-performance deep learning library. In *Proceedings of the 33rd Conference on Neural Information Processing Systems*, pages 8026–8037.

Julia Peyre, Ivan Laptev, Cordelia Schmid, and Josef Sivic. 2017. Weakly-supervised learning of visual relations. In *Proceedings of the 2017 IEEE International Conference on Computer Vision*, pages 5189–5198.

Pouya Pezeshkpour, Liyan Chen, and Sameer Singh. 2018. Embedding multimodal relational data for knowledge base completion. In *Proceedings of the 2018 Conference on Empirical Methods in Natural Language Processing*, pages 3208–3218.

Fereshteh Sadeghi, Santosh Kumar Divvala, and Ali Farhadi. 2015. VisKE: Visual knowledge extraction and question answering by visual verification of relation phrases. In *Proceedings of the 2015 IEEE Conference on Computer Vision and Pattern Recognition*, pages 1456–1464.

Anjany Sekuboyina, Daniel Oñoro-Rubio, Jens Kleesiek, and Brandon Malone. 2019. A relational-learning perspective to multi-label chest x-ray classification. In *Proceedings of the 2021 IEEE 18th International Symposium on Biomedical Imaging*, pages 1618–1622.

Robyn Speer, Joshua Chin, and Catherine Havasi. 2017. ConceptNet 5.5: An open multilingual graph of general knowledge. In *Proceedings of the 31st AAAI Conference on Artificial Intelligence*, pages 4444–4451.

Nitish Srivastava, Geoffrey Hinton, Alex Krizhevsky, Ilya Sutskever, and Ruslan Salakhutdinov. 2014. Dropout: A simple way to prevent neural networks from overfitting. *Journal of Machine Learning Research*, 15(56):1929–1958.

Zhiqing Sun, Zhi-Hong Deng, Jian-Yun Nie, and Jian Tang. 2019. RotatE: Knowledge graph embedding by relational rotation in complex space. In *Proceedings of the 7th International Conference on Learning Representations*.

Kristina Toutanova and Danqi Chen. 2015. Observed versus latent features for knowledge base and text inference. In *Proceedings of the 3rd Workshop on Continuous Vector Space Models and their Compositionality*, pages 57–66.

Ashish Vaswani, Noam Shazeer, Niki Parmar, Jakob Uszkoreit, Llion Jones, Aidan Nicholas Gomez, Łukasz Kaiser, and Illia Polosukhin. 2017. Attention is all you need. In *Proceedings of the 31st Conference on Neural Information Processing Systems*, pages 5998–6008.

Meng Wang, Sen Wang, Han Yang, Zheng Zhang, Xi Chen, and Guilin Qi. 2021. Is visual context really helpful for knowledge graph? a representation learning perspective. In *Proceedings of the 29th ACM International Conference on Multimedia*, pages 2735–2743.

Zikang Wang, Linjing Li, Qiudan Li, and Daniel Zeng. 2019. Multimodal data enhanced representation learning for knowledge graphs. In *Proceedings of the 2019 International Joint Conference on Neural Networks*, pages 1–8.

Ruobing Xie, Zhiyuan Liu, Huanbo Luan, and Maosong Sun. 2017. Image-embodied knowledge representation learning. In *Proceedings of the 26th International Joint Conference on Artificial Intelligence*, pages 3140–3146.

Bishan Yang, Wen tau Yih, Xiaodong He, Jianfeng Gao, and Li Deng. 2015. Embedding entities and relations for learning and inference in knowledge bases. In *Proceedings of the 3rd International Conference on Learning Representations*.

Alireza Zareian, Svebor Karaman, and Shih-Fu Chang. 2020. Bridging knowledge graphs to generate scene graphs. In *Proceedings of the 16th European Conference on Computer Vision*, pages 606–623.

Rowan Zellers, Yonatan Bisk, Ali Farhadi, and Yejin Choi. 2019. From recognition to cognition: Visual commonsense reasoning. In *Proceedings of the 2019 IEEE/CVF Conference on Computer Vision and Pattern Recognition*, pages 6713–6724.

Yu Zhao, Xiangrui Cai, Yike Wu, Haiwei Zhang, Ying Zhang, Guoqing Zhao, and Ning Jiang. 2022. MoSE: Modality split and ensemble for multimodal knowledge graph completion. In *Proceedings of the 2022 Conference on Empirical Methods in Natural Language Processing*, pages 10527–10536.

Xiangru Zhu, Zhixu Li, Xiaodan Wang, Xueyao Jiang, Penglei Sun, Xuwu Wang, Yanghua Xiao, and Nicholas Jing Yuan. 2022. Multi-modal knowledge graph construction and application: A survey. *IEEE Transactions on Knowledge and Data Engineering*, pages 1–20.

Appendix

A Details about Constructing and Validating VTKGs

As described in Section 3.2, we examined all triplets in VRD, UnRel, HICO-DET, VisKE, and ConceptNetW to map each entity and relation to a synset in WordNet (Miller, 1995). We developed a data labeling tool shown in Figure 6 that allows a human expert to select the most appropriate synset of each word in a triplet by examining the meaning of each synset and the semantics of the word in context. It took six weeks to examine all the triplets. In the data labeling process, we also verified whether each triplet is valid or not; we removed the invalid or hard-to-interpret triplets from our datasets, e.g., ⟨`mechanic`, `winter`, `car`⟩. During this process, 269 triplets were removed among 19,065 original triplets. When we sampled 2,000 triplets and double-checked the labels, the labeling accuracy was 95.01%.

Additionally, we checked the matching of each triplet and its image. In our datasets, 1,316 triplets are expressed by images, and there are 141,247 images for triplets. The triplet images came from VRD, UnRel, and HICO-DET. To examine whether a triplet is well matched with its image, we randomly sampled 100 images for each triplet. If a triplet has less than 100 images, we examined all the images for the triplet. As a result, we examined 36,919 images, and each image was examined by two different annotators. We consider a triplet is matched with its image only if both annotators agree on it, i.e., if one of the annotators disagrees, we consider the triplet is not matched with its image. When measuring the matching degree in this way, the accuracy was 98.62%.

When constructing our VTKG datasets, we did not use FB15K237 because FB15K237 delivers a different level of information from VRD, UnRel, HICO-DET, VisKE, ConceptNetW, and WN18RR++. For example, while VTKG-C contains generic relationships between concepts, e.g., ⟨`person`, `write`, `story`⟩, most triplets in FB15K237 provide specific details about particular individuals or facts, e.g., ⟨`James_Cameron`, `graduate_from`, `California_State_University`⟩.

We provide some examples of the triplets and their images and descriptions in our VTKG datasets. As explained above, each entity or relation is represented using a synset of WordNet, e.g., 'airplane.n.01' or 'have.v.01', where 'n' indicates a noun, 'v' indicates a verb, and the last two digits indicate the sense number. The descriptions of entities and relations are from WordNet. Figure 7 shows some examples of triplets in our VTKG datasets.

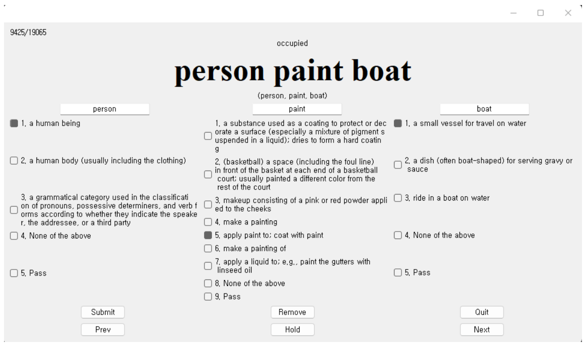

9425/19065

occupied

person paint boat

(person, paint, boat)

person

- [✓ 1. a human being]
- 2. a human body (usually including the clothing)
- 3. a grammatical category used in the classification of pronouns, possessive determiners, and verb forms according to whether they indicate the speaker, the addressee, or a third party
- 4. None of the above
- 5. Pass

paint

- 1. a substance used as a coating to protect or decorate a surface (especially a mixture of pigment suspended in a liquid); dries to form a hard coating
- 2. (basketball) a space (including the foul line) in front of the basket at each end of a basketball court; usually painted a different color from the rest of the court
- 3. makeup consisting of a pink or red powder applied to the cheeks
- 4. make a painting
- [✓ 5. apply paint to; coat with paint]
- 6. make a painting of
- 7. apply a liquid to; e.g., paint the gutters with linseed oil
- 8. None of the above
- 9. Pass

boat

- [✓ 1. a small vessel for travel on water]
- 2. a dish (often boat-shaped) for serving gravy or sauce
- 3. ride in a boat on water
- 4. None of the above
- 5. Pass

Figure 6: Interface of our data labeling tool for mapping each word to the most appropriate synset and also checking the validity of each triplet.

Merging triplets from different sources

One of the critical points of creating VTKGs is properly combining triplets from different sources. Since triplets from different sources are usually written using different vocabularies, as discussed in Section 3.2, we had to find a way to consolidate those vocabularies. To resolve this issue, we replace each entity/relation in a triplet with a synset ID defined in WordNet to express triplets using the vocabulary defined in WordNet. An alternative method we considered was to replace each entity/relation with a word defined in the Cambridge Dictionary. However, using the Cambridge Dictionary resulted in creating redundant triplets due to various synonyms, failing to merge semantically identical triplets. Therefore, we decided to use WordNet synsets when we merge triplets.

B Experimental Details about Running the Baseline Methods

We run baseline methods using GeForce RTX 2080 Ti or RTX A6000 depending on the dependency of each method. For all methods, we use the default hyperparameters provided in their implementations unless otherwise stated. We choose the best configuration for each method based on the validation results. In what follows, we use the notation of the original papers.

For ANALOGY (Liu et al., 2017), we tried

⟨Head Entity,	Relation,	Tail Entity⟩	Image #1	Image #2
⟨airplane.n.01, an aircraft that has a fixed wing and is powered by propellers or jets	**have.v.01,** have or possess, either in a concrete or an abstract sense	**wheel.n.01⟩** a simple machine consisting of a circular frame with spokes (or a solid disc) that can rotate on a shaft or axle (as in vehicles or other machines)		
⟨kite.n.03, plaything consisting of a light frame covered with tissue paper; flown in wind at end of a string	**fly.v.01,** travel through the air; be airborne	**sky.n.01⟩** the atmosphere and outer space as viewed from the earth		
⟨person.n.01, a human being	**drive.v.01,** operate or control a vehicle	**car.n.01⟩** a motor vehicle with four wheels; usually propelled by an internal combustion engine		

Figure 7: Examples of Triplets in VTKGs

the learning rate $\in \{0.001, 0.005, 0.01, 0.05, 0.1\}$ and $\lambda \in \{0.001, 0.005, 0.01, 0.05, 0.1\}$. We tuned ComplEx-N3 (Lacroix et al., 2018) using the regularization coefficient $\in \{0.0, 0.01, 0.05, 0.1, 0.2\}$. In RotatE (Sun et al., 2019) and PairRE (Chao et al., 2021), we tried the learning rate $\in \{0.00005, 0.0001\}$ and $\gamma \in \{6.0, 9.0, 12.0\}$. RSME (Wang et al., 2021) is tuned with the learning rate $\in \{0.005, 0.01, 0.05\}$ and the regularization coefficient $\in \{0.05, 0.1, 0.15, 0.2\}$. We tuned TransAE (Wang et al., 2019) with $\lambda \in \{0.00005, 0.0001, 0.0005, 0.001, 0.01\}$ and $\gamma \in \{2.0, 2.5, 5.0, 7.5, 10.0\}$. In MKGformer (Chen et al., 2022), we tried the learning rate $\in \{0.00005, 0.0005\}$ in the fine-tuning stage. When we ran MKGformer, we had to decrease the batch size from 96 to 32 due to the memory constraint of our GPUs. For OTKGE (Cao et al., 2022), we tried the batch size $\in \{2000, 5000\}$ and the regularization coefficient $\in \{0.001, 0.005\}$. For MoSE (Zhao et al., 2022) and IMF (Li et al., 2023), we used the default parameters provided in their implementations. The results reported in the original IMF paper are not reproducible.

C Hyperparameters of VISTA

In VISTA, the learning rate was set to 0.0001 for VTKG-I and VTKG-C, and 0.001 for WN18RR++ and FB15K237. Unless otherwise stated, the hidden dimension of the transformers was fixed to 2,048. We set $L = 2$, $\widehat{L} = 1$, and $k = \widehat{k} = 1$. The dropout rate of the transformers is 0.1, the dropout rate of the embedding matrices is 0.9, the dropout rate of the textual representation vectors is 0.1, and the step size of the cosine learning rate scheduler is 50. We validated the model performance every 50 epochs.

We tuned VISTA on VTKG-I with $L \in \{2, 3, 4\}$, $\widehat{L} \in \{1, 2, 3\}$, $\widetilde{L} \in \{1, 2\}$, number of attention heads $\in \{2, 4\}$, the dropout rate of the embedding matrices $\in \{0.5, 0.6, 0.7\}$, the dropout rate of the visual representation vectors $\in \{0.3, 0.4\}$, and $k = \widehat{k} \in \{1, 3, 5\}$. We used 768 as the hidden dimension of the transformers, 128 as the batch size, and 0.01 as the dropout rate of the transformers. NVIDIA GeForce RTX 2080 Ti was used to run VISTA on VTKG-I, and it took approximately one minute for a single run with the best hyperparameters.

For VTKG-C, VISTA was tuned with $\widetilde{L} \in \{1, 2\}$, number of attention heads $\in \{2, 4\}$, the dropout rate of the visual representation vectors $\in \{0.3, 0.4\}$, and the dropout rate of the textual representation vectors $\in \{0.0, 0.1\}$. We set the batch size to be 512, $k = \widehat{k} = 3$, and set the dropout rate of the transformers to be 0.01. NVIDIA GeForce RTX 3090 was used to run VISTA on VTKG-C, and it took approximately three hours for a single run with the best hyperparameters.

We tuned VISTA on WN18RR++ with number of attention heads $\in \{8, 16\}$, the dropout rate of the visual representation vectors $\in \{0.2, 0.3\}$, the dropout rate of the textual representation vectors $\in \{0.0, 0.1\}$, and the step size of the cosine learning rate scheduler $\in \{50, 100\}$. We set $\widetilde{L} = 1$ and the batch size is 1024. We used NVIDIA GeForce RTX 3090 and NVIDIA RTX A6000 to run VISTA on WN18RR++, and it took approximately 6 hours for a single run with the best hyperparameters.

For FB15K237, VISTA was tuned with $L \in \{1, 2\}$, number of attention heads $\in \{32, 64\}$, the dropout rate of the embedding matrices $\in \{0.8, 0.9\}$, the step size of the cosine learning rate scheduler $\in \{50, 100\}$, and the batch size $\in \{512, 1024\}$. We set the dropout rate of the visual representation vectors and the textual representation vectors to 0.3 and 0.0, respectively, and $\widetilde{L} = 1$. We used NVIDIA GeForce RTX 3090 and NVIDIA RTX A6000 to run VISTA on FB15K237, and it took approximately 15 hours for a single run with the best hyperparameters.